# $4f$ Delocalization in Gd: Inelastic X-Ray Scattering at Ultrahigh Pressure

B. R. Maddox,[1,2] A. Lazicki,[1,2] C. S. Yoo,[1] V. Iota,[1] M. Chen,[1] A. K. McMahan,[1] M. Y. Hu,[3] P. Chow,[3] R. T. Scalettar,[2] and W. E. Pickett[2]

[1]*Lawrence Livermore National Laboratory, Livermore, California 94551, USA*
[2]*University of California, Davis, California 95616, USA*
[3]*HP-CAT, Advanced Photon Source, Argonne National Laboratory, Argonne, Illinois 60439, USA*

(Received 17 November 2005; published 1 June 2006)

We present resonant inelastic x-ray scattering and x-ray emission spectroscopy results on Gd metal to 113 GPa which suggest Kondo-like aspects in the delocalization of $4f$ electrons. Analysis of the resonant inelastic x-ray scattering data reveals a prolonged and continuous delocalization with volume throughout the entire pressure range, so that the volume-collapse transition at 59 GPa is only part of the phenomenon. Moreover, the $L\gamma_1$ x-ray emission spectroscopy spectra indicate no apparent change in the bare $4f$ moment across the collapse, suggesting that Kondo screening is responsible for the expected Pauli-like behavior in magnetic susceptibility.

DOI: 10.1103/PhysRevLett.96.215701 PACS numbers: 64.70.Kb, 62.50.+p, 64.30.+t, 72.15.Qm

A number of compressed lanthanide and actinide metals exhibit electron correlation driven phase transitions characterized by unusually large volume changes [1–3]. Among the lanthanides, such volume-collapse transitions are seen in Ce (15% volume change), Pr (10%), Gd (5%), and Dy (6%) at pressures of 0.7 [4], 20 [5], 59 [6], and 73 GPa [7], respectively. It is often presumed that the $4f$ electrons delocalize across these collapse transitions due to dramatic changes in properties seen upon going from the large- to small-volume regimes. The crystal structures change from a sequence of high-symmetry structures, observed in metals without $f$ electrons, to low-symmetry early-actinide-like structures, indicative of $f$ bonding [1–3]. The magnetic susceptibility changes from Curie-Weiss behavior reflecting the Hund's rules moments to an expected temperature-independent Pauli-like paramagnetism, suggesting loss of the moments [2,4]. On the other hand, it has been recently shown that Nd reaches a typically itinerant $\alpha$-U structure through a sequence of transitions without any large volume changes [8]. Additionally, high-energy neutron scattering measurements see single-ion magnetic response in the collapsed $\alpha$ phase of Ce [9] in possible disagreement with magnetic susceptibility measurements [4]. It would appear that delocalization in these $f$-electron metals is not fully understood.

There are presently two viable theoretical perspectives which reflect some of these same conflicts. The Kondo volume-collapse (KVC) model for Ce attributes the collapse to a rapid change in the Kondo binding energy with volume associated with screening of the $4f$ moments by the valence electrons [10,11]. While this occurs near the localized limit (large volume) for Ce, implicit in the model is also a prolonged delocalization in the way that the ground state evolves away from sharp $f^1$ character as volume is reduced. Dynamical mean-field theory (DMFT) calculations generally find Kondo-like features in both lanthanides [12] and actinides [13] and specifically support the KVC model for Ce [14], although not necessarily for the other $f$-electron metals [12]. The Mott transition model [15], as exemplified by local density calculations modified to represent the localized regime by spin and orbitally polarized solutions, presents a more abrupt change from localized to itinerant behavior across the collapse transitions, coincident with complete loss of the $f$ moment itself [16–18].

Recent developments in 3rd generation synchrotron x-ray spectroscopies offer new opportunities to clarify the mechanism of delocalization in the $f$-electron metals. This Letter presents resonant inelastic x-ray scattering (RIXS) and x-ray emission spectroscopy (XES) measurements on Gd metal up to 113 GPa, both of which have been used successfully to probe the electronic and magnetic properties of rare-earth and transition-metal compounds [19–24]. In RIXS, we measured the $3d \rightarrow 2p\ L\alpha$ emission after resonant excitation through the Gd $L_{\mathrm{III}}$ edge. The XES experiment consists of measuring the nonresonant $4d \rightarrow 2p\ L\gamma_1$ emission after excitation with high-energy x rays. The results strongly support a Kondo-like scenario by showing (i) a prolonged and continuous (as a function of volume) delocalization of the $4f$ electrons throughout the full pressure range investigated and (ii) a $4f$ moment which does not change at the 59 GPa volume collapse. As in the high-energy neutron scattering results for $\alpha$-Ce [9], it is argued that the XES process measures a bare $4f$ moment and that any moment loss deduced from the magnetic susceptibility must then come from screening by the valence electrons.

Gadolinium foil (99.99%, Alfa Aesar) was used for both the RIXS and XES experiments together with mineral oil as a pressure medium and small ruby chips for pressure determination. Samples were loaded into Livermore-designed piston-cylinder diamond anvil cells fitted with either 300 $\mu$m culet diamonds for low pressure data ($<$60 GPa) or beveled culet diamonds (100 $\mu$m flats inside

 

300 $\mu$m bevels) for high pressure data (>60 GPa). X-ray spectroscopic data were collected at Sector 16 ID-D of the Advanced Photon Source, using an incident x-ray beam microfocused to $20 \times 50$ $\mu$m by a pair of 1 m long Kirkpatrick-Baez mirrors. For RIXS experiments, the incident x-ray energy $\Omega$ was tuned from 7235 to 7257 eV in steps of 2 eV using a diamond double-crystal monochromator. At each incident energy, an $L\alpha_1$ emission spectrum was collected 90° from the incident x-ray beam through a Be gasket. The cell was tilted to ~7° from the horizontal plane to increase the physical cross section of the sample and to minimize the effects of self-absorption. For XES, we used a 12 keV x-ray beam incident through the diamond anvils for nonresonant excitation and collected the $L\gamma_1$ x-ray emission from the sample through a Be gasket, 90° from the incident beam. In both cases, energy analysis was performed using a 1 m Rowland circle spectrometer arranged in the vertical plane. A spherically bent Si(333) single crystal analyzer (100 $\mu$m in diameter) was used to refocus the x-ray emission onto a Si detector (Amp Tek). This configuration provides an energy resolution of approximately 1 eV.

The RIXS spectrum obtained at low pressure is qualitatively similar to that previously obtained from $Gd_3Ga_5O_{12}$ garnet at ambient pressure [20] and is shown in Fig. 1 as a function of energy transfer to the sample ($\Omega - \omega$), where $\omega$ is the emitted x-ray energy. The main features of the spectra are illustrated in the inset in Fig. 1 and consist of a strong peak at $(\Omega - \omega) = 1186$ eV, which resonates at $\Omega = 7247$ eV, corresponding to the dipole-allowed (E1, peak B) $2p \rightarrow 5d$ transition, and a substantially weaker quadrupolar (E2, peak A) peak at $(\Omega - \omega) = 1180$ eV, which resonates at a slightly lower energy of $\Omega = 7239$ eV. This latter feature, which corresponds to the quadrupolar $2p \rightarrow 4f$ transition, illustrates the power of RIXS in resolving weak features normally hidden in x-ray absorption spectroscopy by the much stronger hole-broadened $2p \rightarrow 5d$ transition. The broad peak at $(\Omega - \omega) \sim 1191$ eV exhibits the same resonance characteristics as peak B and is therefore part of the same multiplet [20]. Peak B shows a slight shift with incident energy due to a strong crystal field, which produces two multiplet groups separated by ~1 eV which resonate at slightly different $\Omega$. Incident energies above $\Omega = 7247$ eV correspond to excitations into continuum states and represent nonresonant XES.

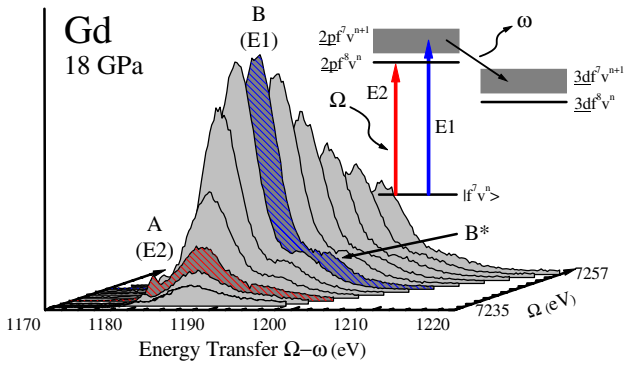


FIG. 1 (color online). RIXS spectra of Gd at 18 GPa taken at a series of incident energies from $\Omega = 7235$ eV to $\Omega = 7257$ eV in steps of 2 eV. The inset shows a schematic energy diagram illustrating the RIXS process for the $2d \rightarrow 4f$ (E2, peak A) and $2p \rightarrow 5d$ (E1, peaks B and B*) features.

With further application of pressure, however, changes in the RIXS spectra occur as shown in Fig. 2(a). Gaussian decompositions of the $\Omega = 7239$ eV spectra taken at each pressure reveal a new feature (peak C) positioned 4.96 eV below peak B emerging at high pressure. The characteristics of this new peak in energy, intensity, and bandwidth are strikingly similar to those previously observed with RIXS during the pressure-induced valence change in YbS ($f^{14}$ in $Yb^{2+}$ and $f^{13}$ in $Yb^{3+}$) [25] and during the $\gamma$-$\alpha$ transition in the Ce alloys [21,22]. The situation is illustrated by the ground-state wave function

$$|\Psi\rangle = \alpha|4f^7\upsilon^3\rangle + \beta|4f^8\upsilon^2\rangle + \gamma|4f^6\upsilon^4\rangle, \qquad (1)$$

where $\upsilon$ signifies valence electrons. In the strongly localized limit, the occupation of the $4f$ shell in Gd is pinned at $f^7$. Under compression, however, the growing $f$-valence hybridization increasingly favors fluctuations of the $4f$ electrons into valence states, and vice versa, resulting in the growth of $f^6$ and $f^8$ components of the wave function at the expense of the predominant $f^7$ character. This type of delocalization differs from intermediate valence, where one stays near the localized limit except that the energies of two different $f$ occupations happen to move closer

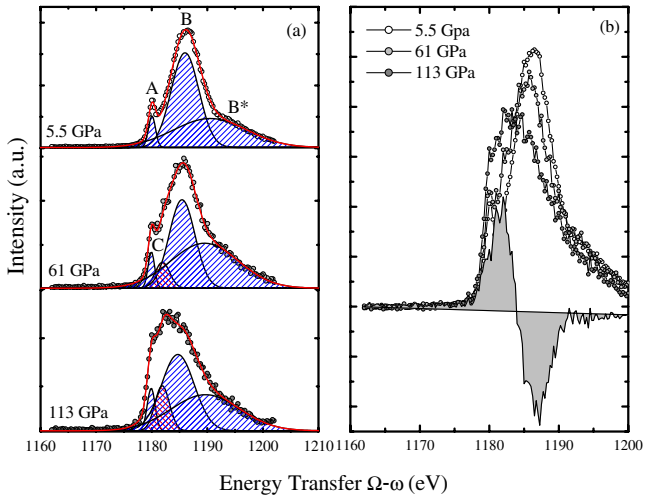


FIG. 2 (color online). (a) RIXS spectra obtained at the $2p \rightarrow 4f$ resonance ($\Omega = 7239$ eV) taken at 5.5, 61, and 106 GPa, together with Gaussian decompositions showing the emergence of a new feature (peak C) at high pressure. (b) Normalized RIXS spectra at the same 3 pressures along with the difference spectrum (shaded) between 113 and 5.5 GPa.

together as a function of a variable such as pressure. Nevertheless, the RIXS process for these two phenomena are similar in that the $4f$ core-hole attraction in the intermediate state puts the peak arising from dipole excitation of the component with larger $f$ occupation ($\underline{2p}4f^8\upsilon^3$, C) at lower energy transfer than that of the smaller occupation ($\underline{2p}4f^7\upsilon^4$, B). Indeed, the interpretations and relative locations of all three peaks A, B, and C in the present study are consistent with the YbS intermediate valence case [Fig. 4(b) in Ref. [25]].

Considering the ground-state wave function given in Eq. (1), the progress of $4f$ delocalization can be quantified by the ratio $|\beta|^2/|\alpha|^2 \approx n(f^8)/n(f^7)$. This ratio can be approximately extracted from the RIXS data by subtracting the lowest pressure $\Omega = 7239$ eV spectrum from each of the higher pressure $\Omega = 7239$ eV scans after normalizing the total area of each spectrum. Figure 2(b) illustrates the procedure by showing the difference spectrum at 113 GPa along with the four $\Omega = 7239$ RIXS scans from Fig. 2(a) after normalization. The positive peak in the difference spectrum was integrated to derive the area $\mathcal{A}$, and the quantity $n(f^8)/n(f^7) \approx \mathcal{A}/(1-\mathcal{A})$ was then calculated. The results are plotted in Fig. 3 as a function of volume, along with recent DMFT results for Ce [12] and experimental values for the ambient-pressure $\alpha$ and $\gamma$ phases of Ce alloys also obtained from RIXS [21]. In both cases, the two volume-collapse regions are shaded. The present data show an approximately continuous and exponential dependence on volume as predicted by theory [12], with the $n(f^{n+1})/n(f^n)$ ratio for Gd ($n = 7$) lying far below that of the Ce ($n = 1$) alloys. This method ignores any $f^6$ contribution to the difference spectra which would occur at higher energy but cannot be resolved from our data. Nevertheless, even if $|\gamma|^2 \approx |\beta|^2$ then this would lead to, at worst, a 25% error in $n(f^8)/n(f^7)$ and, with only minor effects on a semilog scale, would have no impact on our conclusions.

One would expect Gd to be more localized and thus have a smaller $n(f^{n+1})/n(f^n)$ ratio than Ce at the same volume, since the $f$ shell is more tightly bound in the heavier lanthanides due to the ever-increasing but incompletely screened nuclear charge. More important is the half-filled shell in Gd with total $4f$ spin $S = 7/2$ and the associated large impact of the intra-atomic exchange. This is reflected in an energy splitting of ~12 eV (an effective Hubbard U) between lower and upper Hubbard bands in Gd as compared to ~6 eV in Ce [26], which should make Gd significantly more localized. It is interesting to note that the volume-collapse transitions (shaded regions) occur in roughly the same range of $n(f^{n+1})/n(f^n)$ as measured by RIXS in both Gd and Ce.

We have also examined the $f$-electron moment using $4d \rightarrow 2p$ $L\gamma_1$ XES measurements on Gd at high pressure. The intra-atomic exchange interactions between $4f$ and core orbitals lead to a low energy satellite as seen in

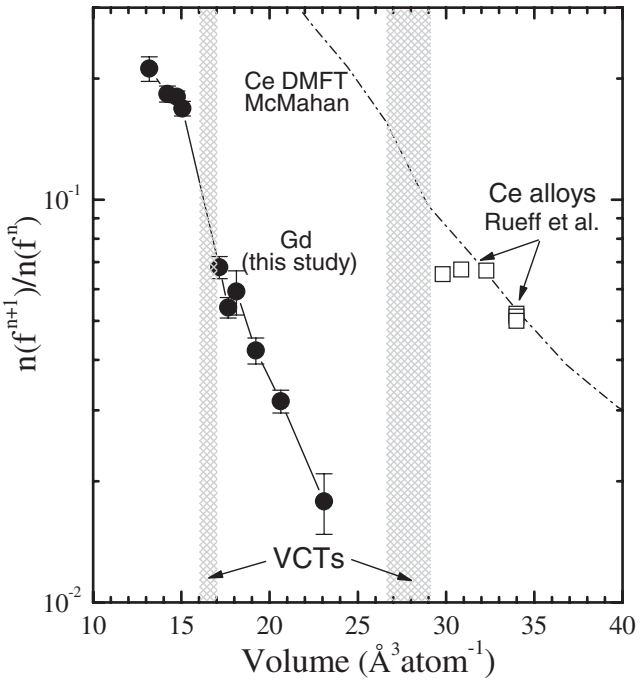


FIG. 3. The degree of $f$-electron hybridization, reflected by the ratio $n(f^{n+1})/n(f^n)$, measured by the present RIXS experiments on Gd compared with those previously determined in RIXS experiments on Ce alloys [21] and in recent DMFT calculations [12]. The volume-collapse transition (VCT) regions for Gd and Ce are shown as hatched areas.

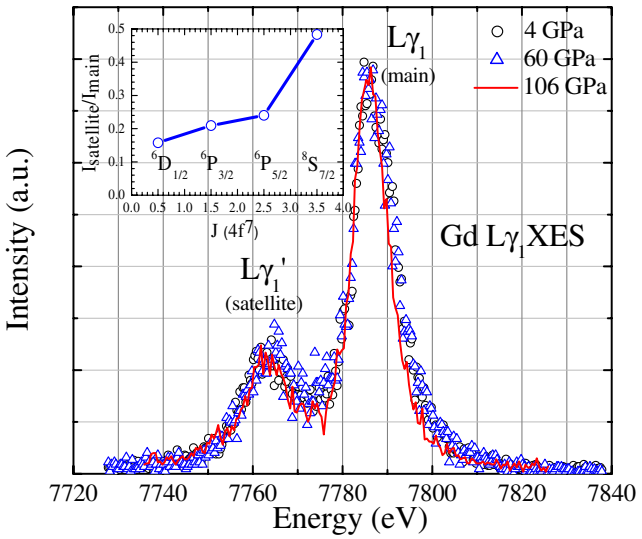


FIG. 4 (color online). $L\gamma_1$ XES spectra of Gd at 4, 60, and 106 GPa, normalized to the main peak intensity, showing no apparent change in the $L\gamma_1'$ satellite peak intensity, suggesting no changes in the $4f$ moments up to 106 GPa. The inset shows $I_{\text{satellite}}/I_{\text{main}}$ derived from calculated $L\gamma_1$ XES spectra, demonstrating that the intensity ratio of the satellite peak to the main peak decreases as you move away from the Hund's rule ground state.

Fig. 4, whose relative height and separation from the main peak should reflect the size of the $4f$ moment [23]. We find no significant change in the $L\gamma_1$ emission spectra up to our maximum pressure of 106 GPa, which suggests no changes in the $4f$ moments up to this pressure and, in particular, no changes across the collapse transition at 59 GPa. The inset in Fig. 4 shows the relative height of the satellite to the main peak obtained from *ab initio* atomic calculations of the XES process for Gd, carried out for the lowest-energy states of the $4f^7$ shell for each of $J = 1/2$, $3/2$, $5/2$, and $7/2$ [27]. This ratio will be smaller in the solid due to screening of the intra-atomic exchange interactions. However, the essential message is that theory predicts that changes away from the $J = 7/2$, ${}^8S_{7/2}$ Hund's rules ground state should result in significant changes in the XES spectra which are not seen experimentally. This behavior is in contrast to the essentially complete loss of Mn $3d$ moment across the Mott transition in MnO as probed by similar $3p \rightarrow 1s$ $K\beta$ XES measurements [24].

As noted earlier, measurements of magnetic susceptibility in $\alpha$-Ce and early actinide analogs have led to the expectation of a temperature-independent magnetic susceptibility in the collapsed phases of the $f$-electron metals, suggesting the absence of moments [2,4]. Yet the single-ion magnetic response seen in high-energy neutron scattering measurements for $\alpha$-Ce is consistent with a still extant $4f$ moment [9], a dilemma which is resolved by the Kondo perspective that the susceptibility measures a $4f$ moment largely screened away by the valence electrons [10,11]. It seems intuitively clear that the primarily atomic XES process, which reflects exchange interactions between $4f$ and core-hole orbitals whose radial distributions lie generally closer to the nucleus than do those of the valence orbitals, is also measuring a bare $4f$ moment. The persistence of such a bare $4f$ moment in Gd through the collapse transitions is therefore consistent with Kondo-like behavior.

In summary, $f$-electron delocalization at high pressure in Gd is brought about by growing hybridization, which causes increasing fluctuations away from the sharp $f^n$ character of the localized limit, and the degree of hybridization can be quantitatively probed by RIXS at pressures exceeding 100 GPa. The process is prolonged and continuous as a function of volume. This, in turn, suggests that the volume-collapse transition is only part of the phenomenon and acts to accelerate the delocalization. The present XES results suggest that the bare $4f$ moment persists across the collapse transition in Gd so that any loss of temperature dependence in the magnetic susceptibility is then likely to arise from Kondo-like screening of the moments.

This work has been supported by the LDRD-04-ERD-020 and PDRP programs at the LLNL, University of California, under the auspices of the U.S. DOE under Contract No. W-7405-ENG-48 and by the Stewardship Science Academic Alliance Program under DOE Grant No. DE-FG01-06NA26204. Use of the HP-CAT facility was supported by DOE-BES, DOE-NNSA (CDAC, LLNL, UNLV), NSF, DOD-TACOM, and the W. M. Keck Foundation.

[1] W. B. Holzapfel, J. Alloys Compd. **223**, 170 (1995).
[2] A. K. McMahan *et al.*, J. Comput.-Aided Mater. Des. **5**, 131 (1998).
[3] A. Lindbaum *et al.*, J. Phys. Condens. Matter **15**, S2297 (2003).
[4] D. G. Kiskimaki and J. K. A. Gschneidner, *Handbook on the Physics and Chemistry of Rare Earths* (North-Holland, Amsterdam, 1978).
[5] B. J. Baer *et al.*, Phys. Rev. B **67**, 134115 (2003); N. C. Cunningham *et al.*, Phys. Rev. B **71**, 012108 (2005).
[6] H. Hua *et al.*, Rev. High Pressure Sci. Technol. **7**, 233 (1988).
[7] R. Patterson, C. K. Saw, and J. Akella, J. Appl. Phys. **95**, 5443 (2004).
[8] G. N. Chesnut and Y. K. Vohra, Phys. Rev. B **61**, R3768 (2000).
[9] A. P. Murani *et al.*, Phys. Rev. Lett. **95**, 256403 (2005).
[10] J. W. Allen and R. M. Martin, Phys. Rev. Lett. **49**, 1106 (1982).
[11] M. Lavagna, C. Lacroix, and M. Cyrot, Phys. Lett. **90A**, 210 (1982).
[12] A. K. McMahan, Phys. Rev. B **72**, 115125 (2005).
[13] S. Y. Savrasov, G. Kotliar, and E. Abrahamas, Nature (London) **410**, 793 (2001).
[14] K. Held, A. K. McMahan, and R. T. Scalettar, Phys. Rev. Lett. **87**, 276404 (2001); M. B. Zölfl *et al.*, Phys. Rev. Lett. **87**, 276403 (2001).
[15] B. Johansson, Philos. Mag. **30**, 469 (1974).
[16] O. Eriksson, M. S. S. Brooks, and B. Johansson, Phys. Rev. B **41**, R7311 (1990).
[17] A. Svane *et al.*, Phys. Rev. B **56**, 7143 (1997).
[18] P. Soderlind and A. Landa, Phys. Rev. B **72**, 024109 (2005).
[19] A. Kotani and S. Shin, Rev. Mod. Phys. **73**, 203 (2001); A. Kotani, Eur. Phys. J. B **47**, 3 (2005).
[20] M. H. Krisch *et al.*, Phys. Rev. Lett. **74**, 4931 (1995).
[21] J.-P. Rueff *et al.*, Phys. Rev. Lett. **93**, 067402 (2004).
[22] C. Dallera *et al.*, Phys. Rev. B **70**, 085112 (2004).
[23] K. Jouda, S. Tanaka, and O. Aita, J. Phys. Condens. Matter **9**, 10 789 (1997).
[24] C. S. Yoo *et al.*, Phys. Rev. Lett. **94**, 115502 (2005).
[25] C. Dallera *et al.*, J. Phys. Condens. Matter **17**, S849 (2005).
[26] Y. Baer and W. D. Schneider, *Handbook on the Physics and Chemistry of Rare Earths* (Elsevier Science, New York, 1987), Vol. 10.
[27] The $4d \rightarrow 2p$ XES process for an isolated Gd atom was calculated using a fully relativistic multiconfiguration Dirac-Fock code with the $4f^7$ shell in its lowest-energy state for $J = 1/2$, $3/2$, $5/2$, and $7/2$ and taking a $J = 1/2$ $2p$ core hole.